Shock wave velocity measurement in the Al_2O_3 under ultrahigh pressure*

Wang Feng(王 峰)[a)†], Peng Xiao-Shi(彭晓世)[a)], Liu Shen-Ye(刘慎业)[a)],
Li Yong-Sheng(李永升)[b)], Jiang Xiao-Hua(蒋小华)[a)], and Ding Yong-Kun(丁永坤)[a)]

[a)] *Research Centre of Laser Fusion, Chinese Academy of Engineering Physics, Mianyang* 621900, *China*
[b)] *Institute of Applied Physics and Computational Mathematics, Beijing* 100088, *China*

(Received 10 September 2010; revised manuscript received 24 February 2011)

In indirect-drive experiment, the blank effect caused by X-rays from Hohlraum will show the dark area in time scale of optical streak camera (OSC). This blank effect, which was a serious problem in indirect-drive shock wave experiments, has been explained by the semiconductor model. The X-rays cause the band to band transition and the probe laser is absorbed by the intraband transition, which leads to a dark region in time scale of the OSC image. In the experiment, the reflectivity of shock wave front was measured to be about 50% at shock wave velocity 32 km/s and was compared to the theoretical calculations with the Drude free electron model. From the experimental data, it is found that the blank effect can be avoided at radiation temperature of 170 eV if the Al layer is thicker than 60 μm.

Keywords: shock wave, optical diagnosis, interfere meter, semiconductor model

PACS: 52.35.Tc, 52.50.Lp, 62.50.+p **DOI:** 10.1088/1674-1056/20/6/065202

1. Introduction

To understand the shock-induced deformation and structural changes at a microscopic level, the dynamics response of different materials to shock loading was extensively studied in the past.[1−3] Most of the shock wave data in transparent material have been achieved in laser-drive experiment and the equation of state (EOS) has been obtained for different kinds of materials such as diamond,[1] quartz,[2] and polystyrene.[3] However, there is the pressure limit for EOS in laser-drive experiment. Since the potential to achieve the ultrahigh pressure (> 1 TPa) in the transparent material, the indirect-drive experiment should be developed.[4−12] Compared with laser-drive experiments, the X-rays generated in Hohlraum reach the target and cause it to absorb the probe laser in transparent material before the shock waves arrive at the target in the indirect-drive experiment.[9,13−16]

As the most important window material, few shock wave data for Al_2O_3 have been reported in indirect-drive experiment. Imaging velocity interferometry system for any reflector (VISAR) has been extensively used to detect and measure laser-driven shock waves in transparent media.[4−12] For imaging VISAR, X-rays generated in Hohlraum cause a brief period of photoionization in the Al_2O_3, which is called the blank effect.[9] The blank effect will lead to a dark area in time scale of optical streak camera (OSC). This blank effect may be an important reason to cause the diagnosis for shock timing to fail at high radiation temperatures (higher than 170 eV).

In this paper, the stream line of experiment setup has been simulated with Multi1D code using quotidian equation of state (QEOS) parameters to obtain the shock wave velocity in Al_2O_3. Then the reflectivity of the shock wave front can be achieved in theoretical simulation. For the direct measuring technique of shock wave velocity, the reflectivity of the shock wave front in Al_2O_3 was provided with experimental data. The Drude-type model has been confirmed in comparison with the experimental data. For the blank effect, the semiconductor model has been used to explain the X-rays photoionization in experimental data. In indirect-drive experiments, the blank effect can be avoided in the time scale and the intensity. With the thick ablator, the blank effect appears and disappears before the shock wave arrives at the transparent material. Then the blank effect can be avoided in time scale. This kind of target can provide the one-shock wave data in indirect-drive experiments.

*Project supported by the National Natural Science Foundation of China (Grant No. 10805041) and the Science and Technology Foundation on Plasma Physics Laboratory (Grant No. 9140C6801021001).

†Corresponding author. E-mail: xiaozei7566@sohu.com

© 2011 Chinese Physical Society and IOP Publishing Ltd

2. Experiment design and Drude model

The plan for achieving the proper shock timing (that is, the proper pulse shape) for laser fusion ignition capsule relies on a diagnostic instrument called VISAR. At its simplest level the active shock breakout (ASBO) diagnosis is a high resolution optical imager that projects a two-dimensional magnified image of the target onto a pair of streak camera detectors (Fig. 1). In somewhat more detail, the system can be divided into a cascade of image relays leading from the target chamber through a 150-mm diagnostic manipulator into the detection paths. The signal passes through a pair of velocity interferometers before being recorded by the streak cameras. The interferometers superimpose a sinusoidal spatial modulation on the image: Doppler shifts in the reflected probe are manifested as shifts of these fringes at the interferometer outputs. The streak cameras record the central chord of the field of view and sweep this signal in time across the output detector. The F number (focal length/diameter) of collecting lens in the chamber is 4.5, which is a compromised result of the collecting efficiency and Doppler shift between the edge of collecting lens and centre of it. The time resolution of the streak camera is 30 ps and the space resolution is 8 μm. The wavelength of laser pulse is 351 nm and the wavelength of probe laser is 532 nm which can avoid the scattering interfering from the 526.5 nm in the chamber with 2-nm FWHM interfere filter.

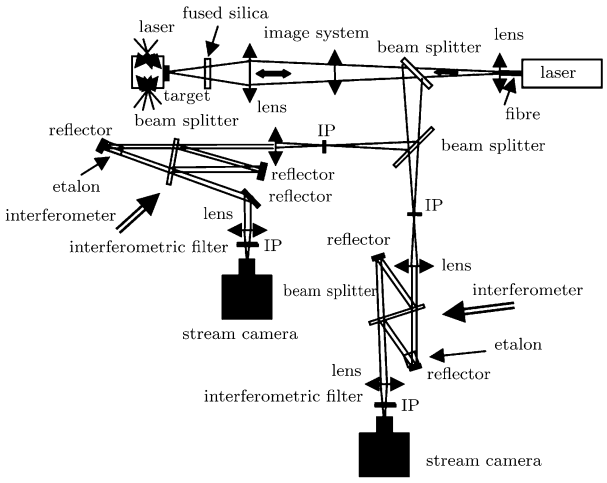


Fig. 1. Schematic diagram of IVISAR system.

Figure 2 shows the diagram of Hohlraum target in our experiment. The 8-way lasers enter the hole; the diagnostic aperture is about 400 μm × 600 μm on the side of Hohlraum target. The ablation layer is of aluminum (Al) with a 60 μm/80 μm step. The Al step (60 μm/80 μm) is attached to the diagnostic aperture of 400 μm × 600 μm with ∼1 μm adhesive. The Al_2O_3 window with 200-μm thickness coated with 1-μm Al on the rear surface is glued on the low step of Al (60 μm). In order to shield the effect of adhesive, there is 1-μm Al coated on the rear side of the transparent window before it was adhered to the Al base. Therefore the interface of aluminum step and the transparent window consists of the Al-adhesive-Al-transparent material. The thickness of adhesive is less than 2 μm which has little effect on shock wave measurement.

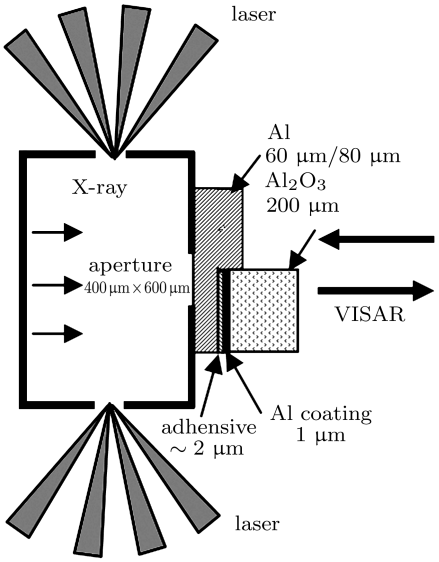


Fig. 2. Schematic diagram of target in our experiment.

Under ultrahigh pressures, all insulators will be expected to transform into metals at high enough compression due to the closing of the energy gap separating the occupied and unoccupied states[1718] in the density of states. Such a pressure-induced gap closure will be preceded by a stage when thermal excitation can excite substantial numbers of electrons across the reduced gap into unoccupied states. For the basic EOS experiment, the technique which can measure the shock wave front directly in the transparent material has been developed in SGIIIYX of China.

Shock wave front reflectivity is much greater than a few percent, which may be a clear indication that the delocalized electrons are present in the shocked liquid. To understand the origin of such delocalized electrons, we first note that for strong shocks, the thermal energy increases much more rapidly than the compressive energy. This process can be explained by

using Fig. 3. When the shock pressure is less than 10^{11} Pa,[17,18] the band gap becomes narrow and the reflectivity of shock wave front is a few percent. From the VISAR, the reflective signal of shock wave front is very small. As the shock pressure increases, the band gap will be closed. Then the shock wave front will reflect the probe laser due to delocalized electrons contributions. For a VISAR system, the important parameter is the reflectivity of shock wave front. To quantitatively describe the reflectivity of shock wave front, we introduce a simple semiconductor model to predict the conduction electron density as a function of temperature, then use electron density in a Drude-type model to determine the dielectric constant and to obtain the reflectivity of the shock wave front.[17,18]

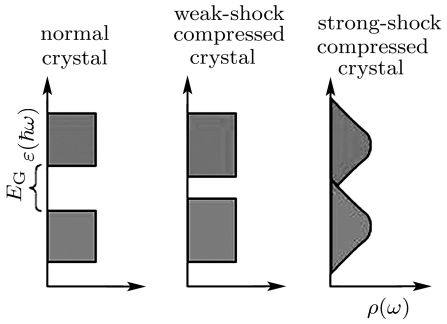


Fig. 3. Variation of band gap with shock pressure.

The number density of conduction electrons in an intrinsic semiconductor is given by $N_e = 2(mk_BT/2\pi\hbar^2)^{3/2}F(-E_g/2k_BT)$, where m is the effective electron mass, k_B is Boltzmann's constant, T is the temperature, E_g is the energy gap in the electronic density of states (which is allowed to vary linearly with mass density) and $F(\eta) = (2/\sqrt{\pi})\int_0^\infty\{\sqrt{x}/[1+\exp(x-\eta)]\}\mathrm{d}x$ is a Fermi-type integral. With this "free" electron density $N_e(T)$ we can determine the relative dielectric constant in Drude-type model from $\varepsilon = \varepsilon_b[1-(\omega_p^2/\omega^2)(1+\mathrm{i}/\omega\tau_e)]$, where ε_b is the contribution due to bound electrons, $\omega = 3.5\times10^{15}$ s^{-1} for 532 nm and τ is the electron relaxation time. The plasma frequency is $\omega_p^2 = N_e e^2/\varepsilon_b\varepsilon_0 m^*$, where N_e is the number of "free" electrons, e is the electron charge, ε_0 is the permittivity of free space and m^* is the reduced mass of the electron, $m_e/2$ characteristic of a semiconductor resulting from the presence of holes.

From Snell laws, the complex index of refraction, given by $n = \sqrt{\varepsilon}$, can be used to calculate the reflectivity from $R = |(n-n_{00})/(n+n_{00})|^2$, where $n_{00} = 1.77$ is the index of unshocked Al_2O_3. The optical reflectivity of the shock wave at 532 nm, defined as the fraction of energy reflected by the moving shock wave front, is shown in Fig. 4. The Hugoniot data of Al_2O_3 is shown in Fig. 5 with QEOS. And the reflective data of shock wave is shown in Fig. 4 with Drude-type model. After we analyse the data in Figs. 4 and 5, the reflectivity is about 44% with the shock wave velocity 32 km/s for Al_2O_3.

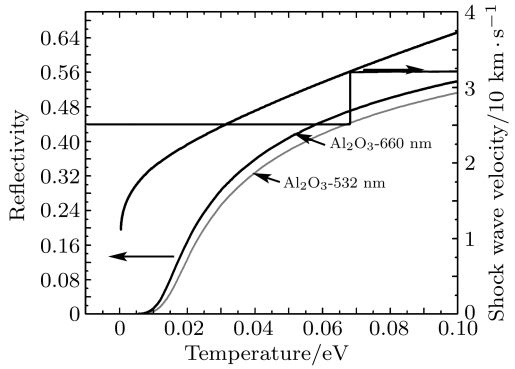


Fig. 4. Calculated relationship of shock wave temperature, velocity and reflectivity in Al_2O_3. The reflectivity of 660 nm is higher than that of 532 nm.

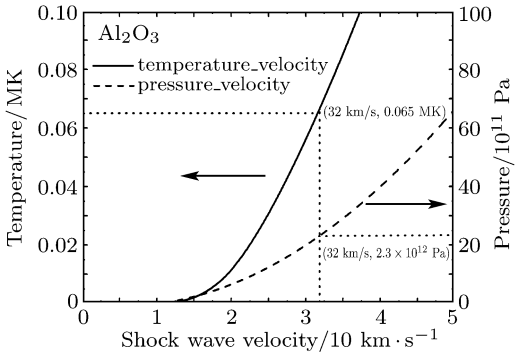


Fig. 5. Hugoniot data for Al_2O_3 with QEOS.

In order to estimate the experimental result, we simulate the compressing process in the Al and Al_2O_3 with laser pulse of 1-ns width (Al is 60 μm and the Tr_{max} is 170 eV). Figure 6 shows the stream line at the 170-eV radiation temperature. The shock wave front will appear in the Al_2O_3 at 2.0 ns, and the interface of Al and Al_2O_3 is behind the shock wave front. From Fig. 7, the shock wave velocity in Al_2O_3 at 2.0 ns is 32 km/s and the shock wave velocity is decelerated after 2.0 ns. Then the reflectivity of shock wave front is about 44%, which is sufficient for VISAR system. From our experience, the critical reflectivity is about 8% for our imaging VISAR. When the shock wave front reflectivity is lower than 8%, the signal is too weak to get the shock wave velocity from the fringe image.

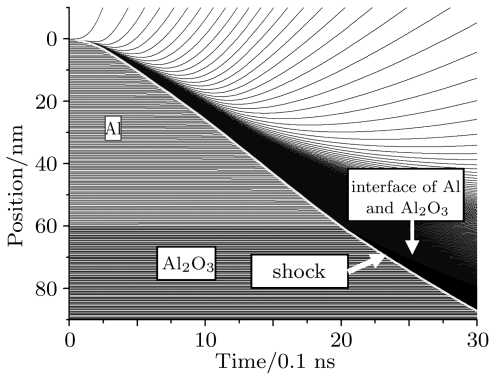


Fig. 6. Stream lines of Al and Al_2O_3 with $Tr = 170$ eV. The thickness of Al is 60 μm, and that of Al_2O_3 is 30 μm.

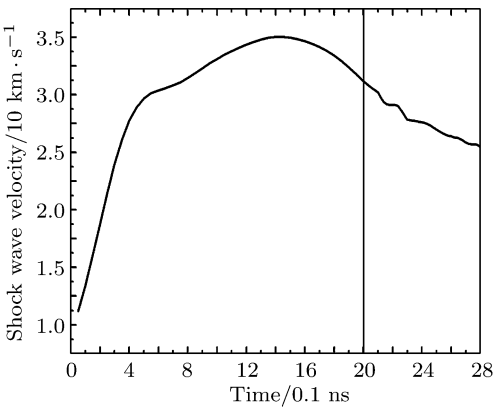


Fig. 7. Shock wave velocity in Al and Al_2O_3 material. The shock wave arrives at the interface at 2.0 ns.

3. Experimental result

Figure 8 shows the experimental signal from the streak camera with Al_2O_3 window. From the experimental data, it is found that there is a dark area in the time scale. The width of the dark area is longer than 1 ns which is the width of the laser pulse. At 2.0 ns, the shock wave is transmitted to the interface between Al layer and Al_2O_3 material. Since the dark area appears before the shock wave arrives at the interface between Al layer and Al_2O_3 material, the blank effect can be avoided by using the 60-μm Al in the time scale. Because the pressure of the shock wave is so high that the delocalized electrons can reflect the probe laser, the fringe jumps suddenly and shifts continuously. The solid line in Fig. 8(b) shows the shock wave trace in Al and Al_2O_3.

Figure 9 shows the velocity curve of the shock wave front in Al_2O_3 obtained with the two sensitivity methods. The etalons of the two arms in VISAR is 4 mm and 7 mm (fused silica), then the fringe sensitivities are 7.29 km·s^{-1}/Fr and 4.16km·s^{-1}/Fr respectively. The two velocity curves are not coincident in Fig. 9 due to the sweep nonlinearity of streak camera in time scale. When the solid line and dashed line match together, the shock wave velocity can be obtained. The shock wave velocity is 32 km/s when the shock wave arrives at the interface between Al and Al_2O_3 and the reflectance ratio is about 50%.

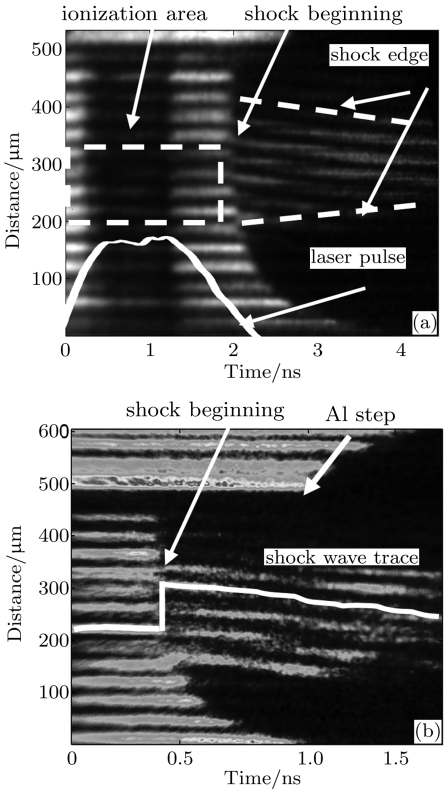


Fig. 8. Recording signal of (a) low sensitivity and (b) high sensitivity. Flat-topping of shot laser pulse is 1 ns with $Tr_{\max} = 170$ eV.

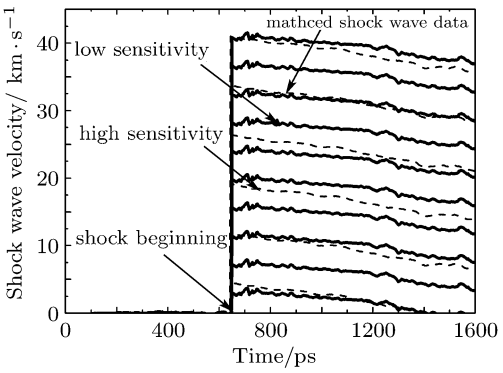


Fig. 9. Data processing result with two sensitivity methods. Solid lines show the high sensitivity data (4.16 km·s^{-1}/Fr). Dashed lines show low sensitivity data (7.29 km·s^{-1}/Fr).

4. Semiconductor model

The blank effect in Fig. 8 can be explained using Fig. 10. The plasma corona excited by X-rays

in the Hohlraum target irradiates the Al_2O_3 which will absorb the probe laser (532 nm) during the shock wave transfer in the Al_2O_3.[9] However, the reflective signal is so weak that the recording system cannot have the high contrast fringe to appear in the dark area as shown in Fig. 8(a). The semiconductor model has been developed to explain the photoionization in Al_2O_3.[9] Figure 11 shows the two steps of X-ray excitation and the free carrier modulation. First, X-rays excite the band to band transition, which means there are too many electrons excited from the valence band to the conduction band. Second, the valence band width which may be wider than 2.33 eV (photo energy, 532 nm) induces the intraband transition excited by the incident probe laser. The valence band in Al_2O_3 will absorb the probe laser when the carrier has been excited by the X-rays from the valence band to conduction band. This transition is called the intraband excitation.

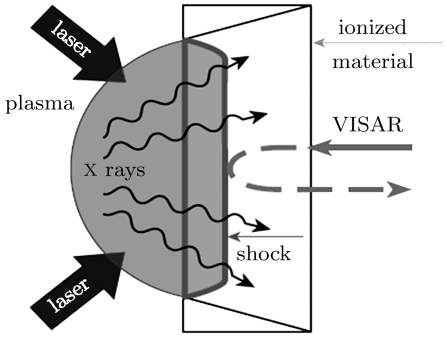


Fig. 10. Diagram of X-ray ionization effect on diagnosis.

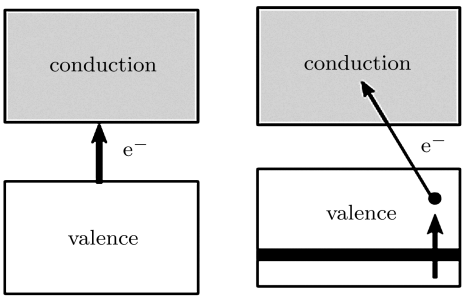


Fig. 11. Two-step semiconductor model of (a) band-to-band transition and (b) intraband transition caused by X-ray.

Figure 12 shows the curves of radiant flux and blank signal versus time. The data in it come from the white block in Fig. 8(a). When the flux reaches the highest value, the blank signal is the lowest at 1.1 ns. At 1.1 ns, the X-rays from Hohlraum excite the band to band transition, which means there are too many electrons excited from the valence band to the conduction band. The valence band in Al_2O_3 will absorb the highest power of probe laser when the carrier has been excited by the X-ray from the valence band to conduction band at 1.1 ns. The blank effect of the signal was in good agreement with the explanation of the semiconductor model.

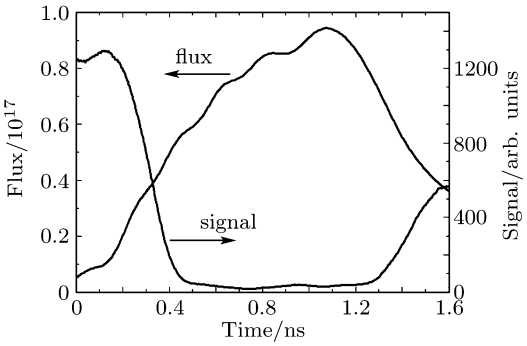


Fig. 12. Relationship of signal intensity and radiant flux.

5. Conclusion

In indirect-drive experiment, X-rays generated in the laser plasma cause a brief period of photoionization in the Al_2O_3, which is called the blank effect. This blank effect will absorb the probe laser to make the shock wave measurement fail. With the semiconductor model, the blank effect can be explained qualitatively. The blank effect can be avoided in the time scale and the intensity. With the thick ablator, the blank effect appears before the shock wave arrives at the transparent material. Then the blank effect can be avoided in time scale. After using the optimized planar target (with the thick ablator), the shock wave data have been achieved in indirect-drive experiment.

When the shock wave arrives at the interface between Al and Al_2O_3, the shock wave velocity is 32 km/s and the reflectance ratio is 50% under the condition of $Tr_{max} = 170$ eV and Al = 60 μm, which is higher than the simulation data 44% in Fig. 4 due to the counting deviation in experimental result. However, the difference of shock wave front reflectivities from the Drude theory and experiment can be accepted because the reflective signal from shock wave front is large for VISAR in the experiment design stage. These experimental data and the Drude theory produce a new way for ultrahigh pressure experiment.

References

[1] Hicks D G, Boehly T R, Celliers P M, Bradley D K, Eggert J H, McWilliams R S, Jeanloz R and Collins G W 2008 *Phys. Rev.* B **78** 174102

[2] McWilliams R S, Eggert J H, Hicks D G, Bradley D K, Celliers P M, Spaulding D K, Boehly T R, Collins G W and Jeanloz R 2010 *Phys. Rev.* B **81** 014111

[3] Ozaki N, Ono T, Takamatsu K, Nakano M, Kataoka T, Yoshida M, Wakabayashi K, Nakai M, Nagai K, Shigemori K, Yamanaka T and Kondo K 2005 *Phys. Plasmas* **12** 124503

[4] Celliers P M, Bradley D K, Collins G W, Hicks D G, Boehly T R and Armstrong W J 2004 *Rev. Sci. Instrum.* **75** 4916

[5] Bradley D K, Eggert J H, Hicks D G, Celliers P M, Moon S J, Cauble R C and Collins G W 2004 *Phys. Rev. Lett.* **93** 195506

[6] Hicks D G, Boehly T R, Celliers P M, Eggert J H, Vianello, Meyerhofer D D and Collins G W 2005 *Phys. Plasmas* **12** 082702

[7] Barker L M and Hollenbach R E 1972 *J. Appl. Phys.* **43** 4669

[8] Smith R F, Eggert J H, Saculla M D, Jankowski A F, Bastea M, Hicks D G and Collins G W 2008 *Phys. Rev. Lett.* **101** 065701

[9] Theobald W, Miller J E, Boehly T R, Vianello E, Meyerhofer D D, Sangste T C, Eggert J and Celliers P M 2006 *Phys. Plasmas* **13** 122702

[10] Chen K G, Zhu W J, Ma W, Deng X L, He H L and Jing F Q 2010 *Acta Phys. Sin.* **59** 1225 (in Chinese)

[11] Wang H Y, Liu J H, Peng G R and Wang W K 2010 *Chin. Phys.* B **19** 096203

[12] Olson R E, Bradley D K, Rochau G A, Collins G W, Leeper R J and Suter L J 2006 *Rev. Sci. Instrum.* **77** 10E523

[13] Huang X G, Fu S Z, Shu H, Ye J J, Wu J, Xie Z Y, Fang Z H, Jia G, Luo P Q, Long T, He J H, Gu Y and Wang S J 2010 *Acta Phys. Sin.* **59** 6394 (in Chinese)

[14] Li Y H, Liu F S, Ma H Y, Cheng X L, Ma X J, Sun Y Y, Zhang M J and Xue X D 2010 *Acta Phys. Sin.* **59** 2104 (in Chinese)

[15] Li X M, Yu Y Y, Li Y H, Zhang L, Ma Y, Wang X S and Fu Q W 2010 *Acta Phys. Sin.* **59** 2691 (in Chinese)

[16] Xi F and Cai L C 2009 *Chin. Phys.* B **18** 2898

[17] Hicks D G, Celliers P M, Collins G W, Eggert J H and Moon S J 2003 *Phys. Rev. Lett.* **91** 035502

[18] Celliers P M, Collins G W, Da Silva L B, Gold D M, Cauble R, Wallace R J, Foord M E and Hammel B A 2000 *Phys. Rev. Lett.* **84** 5564